EGTRIB Journal
JOURNAL OF
THE EGYPTIAN SOCIETY OF TRIBOLOGY
VOLUME 17, No. 4, October 2020, pp. 55 - 69 **ISSN 2090 - 5882**

(Received September 21. 2020, Accepted in final form September 28. 2020) www.egtribjournal.com

STUDY OF ALUMINUM TUBE COLD NOSING PROCESS INTO CONICAL AND HEMI-SPHERICAL DIES WITH DIFFERENT COEFFICIENTS OF FRICTION

Rania Ali Abdelhameed[1*], Samy Zein El-Abden[1], Mohieldeen Abdel-Rahman[1] and Ibrahim M. Hassab-Allah[2]

[1]Department of Production Engineering and Mechanical Design, Minia University, Minia, EGYPT.
[2]Mechanical Engineering Department, Faculty of Engineering, Assuit University, Assuit, EGYPT.
* Corresponding Author E-mail: rania.ali.pg@eng.s-mu.edu.eg

ABSTRACT
Theoretical analysis and finite element method were used to simulate the cold nosing process of commercial purity Aluminum tubes into conical and hemispherical dies. The influences of process parameters, namely initial tube wall thickness, conical semi-die angle were investigated. The effect of surface conditions on the load/displacement curve in the nosing process was investigated. The results of the nosing process were obtained in terms of load-displacement curves, thickness distribution of deformed parts, the nosing ratios and strain distributions. According to these finding, the final shape and defects of the product can also be predicted. Experimental work was carried out to verify the simulation results. A new developed setup design was proposed to improve the product quality. Two adjacent punches were used: one with a front plunger and the other was an outer sleeve to constrain the tube. It could be observed that the load increase with increasing the tube wall thickness and semi die angle. The load increased with increasing the coefficient of friction to overcome friction between the die and tube. The nosing ratio increases as wall thickness increases. Comparison between analytical and FE predictions to the experimental results showed good agreement.

KEYWORDS
Theoretical analysis, Finite element analysis (FEA); Hemispherical die; Conical die; Nosing ratio, Failure modes.

INTRODUCTION
Nosing of tubular materials is one of the popular and simplest processes in the forming of tubes. It is performed by forcing a punch (axial pressing) into the tube end with the die, and then retracting the punch back off after achieving the desired shape. The process has wider applications in the production of the revolution vessels, a connection between tubes, fluid tube circuits, airbags, and guides for shafts in automobile manufacturing and assembly industries.

A new approach was presented to design the shell nosing and modify the initial shape of the die. Simulation and modification the initial shape of the die has led to obtain an optimal perform design zhu [1]. The solutions were studied for performing design in the

shell nosing process. The FEM was used to get two approximate solutions for simplicity and accuracy kobayashi [2]. The perform design and the mechanics of the shell nosing process using FEM simulation. Experiments were conducted on AA 2024 to study the change in geometric and the load required for nosing process. Good agreements were found between numerical and experimental results Tang et al [3]. The recyclable mandrels were used to deform the nosing with thin thickness tubes and leaving it without any defects. A manufacturing process able to fabricate tubes into small size: seamless and reservoirs. The process was carried out by axial pressing the open ends of a tube against two shaped dies, while providing internal support by a mandrel, until achieving the desired shape of the reservoir Alves et al [4].

An innovative extension process was presented to form thin-walled hollow spheres using sacrificial polymer mandrels. The polymer mandrel was utilized to provide an internal support in the tube to get hollow spheres of uniform wall thickness with a single-stage nosing process. Also, they obtained a good agreement between the FE and experimental results Alves et al [5]. An analysis for nosing process using FEM was conducted to study the effect of different parameter on stainless steel tube with conical die. Results were compared and it was concluded that the nosing ratio increased with increasing tube wall thickness, semi-die angle, die fillet radius, length and decreasing with increasing friction factor and strain hardening exponent Kwan et al [6]. The influence of loading rate and performs design in the nosing process was studied into a spherical die. FEM was used to compute the nosing ratio and strain rate distribution in the nosing process compared to theory. The results showed that there was good agreement between theoretical analysis and FEM simulation Lu [7].

The flaring and nosing processes of composite alloy tubes using FEM was analyzed and discussed the effects of thickness ratio, semi die angle and coefficient of friction on forming loads and compared the predicted results with experimental data. Good agreement between the two results was found. The load increases with increasing the coefficient of friction; semi dies angle and thickness ratio Huang [8]. The effect of process parameters was studied on the material forming behavior and forming limits. Thin-walled tubes were compression-bent and nosed. In the case of the nosed part, it was concluded that die contour, initial gap height, tube radius, and friction condition affect forming limits. FEA proved to be capable of generating forming limit diagrams ((FLD's) and determining the critical nosing ratio Gouveia et al [9].

A tool design was developed to suppress the fracture at the tip of the tube after nosing into a die. Investigating the parallel portion on the nosing process, it was noticed that the parallel portion did not prevent the fracture because of the hoop stress Kuboki et al [10]. The cold nosing process was studied by using elasto-plastic and rigid-plastic FEM Results were found to be in agreement with experimental data. The limit of the die penetration depends on the friction along with the interface. The coefficient of friction was increase when the penetration limit was decreased Huang et al [11].

Comprehensive theoretical and experimental investigation was presented of the external inversion of thin-walled tubes using a die. The influence of friction on the process formability, pressurized inside the tube, the displacement of the upper punch plays an important role in the success of the forming operation. Buckling occurred when the tube was long and had a relatively thick thickness. Wrinkling (or local buckling) occurred when the tube was short or long with the thin wall Rosa et al [12]. The influence of cylinder

length was explained on the nonlinear elastic buckling behavior of clamped cylindrical tubes under global bending. It can found that under uniform axial compression the tube length was affected in buckling behavior and strength Rotter et al [13].

The FEM simulation was used to study the effect of the process parameter on the nosing process. It can be observed that load increases with increasing the wall thickness and the semi die angle. Buckling appeared in large semi die angle because of the high contact between the die and the shell Salih and Ismail [14]. The effects of circular curved part at conical die inlet, outer cylindrical guide and local annealing on the nosing limit were investigated Manabe and Nishimura [15]. The nosing limit increased with increase in the outer guide and local annealing. The circular curved part improved the forming limit. Also, local annealing proved to prevent the occurrence of buckling and wrinkling.

An experimental work was conducted to study the defects on low carbon steel sheets. Earing appeared because of different plastic strain ratio at different directions and lead to irregularity on the tip of the cup. High anisotropy caused more earing and decreased the efficiency of the process Tajally et al [16].

The objective of this work is to investigate aluminum tube nosing into a die using conical and hemispherical dies. A modified punch design, including a front plunger part, was introduced to be inserted inside the original tube to enhance axiality. An outer control sleeve was also used to constrain the tube and this led to eliminate bulging which improved the deformation process and avoided the occurrence of defects in the un-deformed part of the tube during the process, giving more product compatibility. The influence of the process parameters; wall thickness, semi-die angle, surface condition and dies shape on the deformation mode, nosing ratio, thickness distribution, strain distribution, and failure type will be checked using the FEA. Setup will be designed and manufactured and tubular specimens will be prepared according to the experimental plan. Experiments will be carried out and experimental results will be compared with the analytical prediction and the FE results.

THEORETICAL ANALYSIS

In order to analyze the deformation process characteristics in nosing process the following assumptions were made:

- **Isothermal and steady-state process.**
- **Uniform friction along with the die-tube interface.**
- **Work-hardening material of the tube is obtained from the compression test.**
- **Levy-Mises stress-strain relations are used in the analysis.**

At die entrance in the tube nosing process Mohammed [17], the tube is bent toward axis under compression, and then begins to flow over the die surface accordingly, compression in circumferential direction occurs. So, there are three stages of deformation exists along the tube during nosing. The compression zone, the free bending zone, and the plastic deformation zone are shown in Figure 1. To get a successful product, one should analyze the influences of the tube nosing parameters namely initial tube wall thickness (to), conical semi-die angle (α), coefficient of friction (μ) and die shape on the deformation mode, critical nosing ratios (CNR's) of the formed tube. Also, failure types are to be checked.

The theoretical analysis for conical die

Figure 1 presents the nosing process and the coordinate systems at conical die with semi die angles (15, 30, 45, 60°).

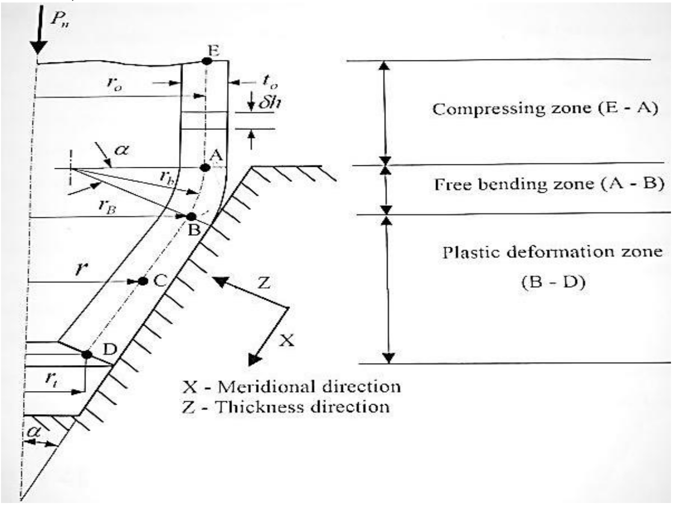

Fig. 1 Nosing die, tube geometry and the coordinate systems Mohammed [17].

1- **The amount of incremental work of bending work at point A**

$$\delta W_B = 4\pi \frac{r_o}{r_b} K1 \delta h \left(\left(\frac{\sqrt{3}\varepsilon_0}{2} + \frac{t_0}{2r_b}\right)^{n+1} \left(\frac{r_b t_0}{2(n+1)}\right) - \left(\frac{\sqrt{3}\varepsilon_0}{2} + \frac{t_0}{2r_b}\right)^{n+2} \left(\frac{{r_b}^2}{(n+1)(n+2)}\right) + \left(\frac{\sqrt{3}\varepsilon_0}{2}\right)^{n+2} \left(\frac{{r_b}^2}{(n+1)(n+2)}\right) \right) \quad (1)$$

2- **The amount of incremental work of unbending work at point B**

$$\delta W_u = 4\pi K1 \frac{r_o}{r_b}\, \delta h \left(\left(\frac{r_b}{(n+1)}\right) \left(\frac{\sqrt{3}\varepsilon_0}{2} + \frac{t_0}{2r_b}\right)^{n+1} \left(\frac{t_0}{2}\right) - \left(\frac{{r_b}^2}{(n+1)(n+2)}\right) \left(\frac{\sqrt{3}\varepsilon_0}{2} + \frac{t_0}{2r_b}\right) + \left(\frac{{r_b}^2}{(n+1)(n+2)}\right) \left(\frac{\sqrt{3}\varepsilon_0}{2}\right)^{n+2} \right) \quad (2)$$

Where, δh is incremental die penetration, and ε_0 is strain.

3- **The friction work in plastic deformation zone (friction zone) B - D**

$$\delta W_F = 2\pi\, \mu\, t_0 r_0 \cot\alpha\, \delta h\, K \left(\frac{2}{\sqrt{3}}\right)^{n+1} \left(\frac{1}{(n+1)}\right) \left(\left(\frac{\sqrt{3}\varepsilon_0}{2} + 1 - \frac{r_t}{r_0} \right)^{n+1} - \left(\frac{\sqrt{3}\varepsilon_0}{2}\right)^{n+1} \right) (3)$$

4- **Tube contraction work**

$$\delta W_C = 2\pi\, t_0 r_0\, K\, \delta h \left(\frac{2}{\sqrt{3}}\right)^{n+1} \left(\frac{1}{(n+1)}\right) \left(\left(\frac{\sqrt{3}\varepsilon_0}{2} + 1 - \frac{r_t}{r_0} \right)^{n+1} - \left(\frac{\sqrt{3}\varepsilon_0}{2}\right)^{n+1} \right) (4)$$

5- Total incremental work

The total incremental work is equal the sum of increment work of bending work, increment work of unbending work, increment work in friction zone, and incremental work of tube contraction work.

$$\delta W_t = \delta W_B + \delta W_u + \delta W_F + \delta W_C \quad (5)$$

Hence,

$$\delta W_t = 8\pi K \left(\frac{2}{\sqrt{3}}\right)^{n+1} \frac{r_o}{r_b} \delta h \left(\left(\frac{\sqrt{3}\varepsilon_0}{2} + \frac{t_0}{2r_b}\right)^{n+1} \left(\frac{r_b t_0}{2(n+1)}\right) - \left(\frac{\sqrt{3}\varepsilon_0}{2} + \frac{t_0}{2r_b}\right)^{n+2} \left(\frac{{r_b}^2}{(n+1)(n+2)}\right)\right) +$$
$$2\pi\, \mu\, t_0 r_0 \cot\alpha\, \delta h\, K\left(\frac{2}{\sqrt{3}}\right)^{n+1} \left(\frac{1}{(n+1)}\right)\left(\left(\frac{\sqrt{3}\varepsilon_0}{2} + \quad 1 - \frac{r_t}{r_0}\right)^{n+1} - \left(\frac{\sqrt{3}\varepsilon_0}{2}\right)^{n+1}\right) +$$
$$2\pi\, t_0 r_0\, K\, \delta h \left(\frac{2}{\sqrt{3}}\right)^{n+1} \left(\frac{1}{(n+1)}\right)\left(\left(\frac{\sqrt{3}\varepsilon_0}{2} + 1 - \frac{r_t}{r_0}\right)^{n+1} - \left(\frac{\sqrt{3}\varepsilon_0}{2}\right)^{n+1}\right) \quad \textbf{(6)}$$

6- Nosing load

The load required to cause tube nosing (P_n) is equal the total incremental work derived by the incremental die penetration.

$$P_n = \frac{\delta W_t}{\delta h} \quad \textbf{(7)}$$

$$P_n = 8\,\pi\, K r_o \left(\frac{2}{\sqrt{3}r_b}\right)^{n+1} \left(\frac{t_0}{2}\right)^{n+2} \left(\frac{1}{(n+2)}\right) +$$
$$2\pi\, t_0 r_0 K\left(\frac{2}{\sqrt{3}}\right)^{n+1} \left(\frac{1}{(n+1)}\right)\left(\left(1 - \frac{r_t}{r_0}\right)^{n+1}\right)(1 + \mu\cot\alpha) \quad \textbf{(8)}$$

Where, r_o is the initial mean radius, r_b is the bending radius, t_o the mean thickness, μ is the coefficient of friction, α is the semi die angle, K is the strength coefficient, and n is the strain hardening exponent is a function of the material true stress- true strain relation.

2.1 The theoretical analysis for hemispherical die

Figure 2 shows the nosing process for Aluminum tube at hemispherical die with die radius 24.1 mm, and the tube geometry in table 1 Amirhosseini et al, [18].

1- Tube contraction work (Ec) (circumferential work)

$$E_c = 2\pi\, \sigma_0 r_1^2 t_o \left(\alpha - \frac{2R_o - t}{2R_o - t_o} \sin\alpha\right)$$
(9)

$$r_1 = R_o - \frac{t_o}{2} \quad , \qquad r_2 = \left(R_o - \frac{t_o}{2}\right)\cos\alpha$$
(10)

$$t = R_o - \sqrt{{R_o}^2 - \frac{2r_1 t_o}{\cos\alpha}} \quad \textbf{(11)}$$

2- The bending work (EB)

Bending work at tube end

$$E_B = \frac{\pi \sigma_o r_1 t^2}{2} \sin\alpha \quad \textbf{(12)}$$

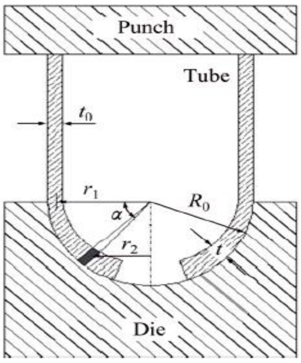

Fig. 2: Nosing process using hemispherical die Amirhosseini et al, [18].

3- The amount of unbending work (Eu)

During the nosing process, bending progress (meridian strain) occurs in the longitudinal direction of tube wall and unbending progress occurs in the circumferential direction. Dissipated work by the meridian strain is equal to dissipated strain work by the bending process due to the spherical geometry, so

$$E_B = E_u \quad (13)$$

4- The friction work in plastic deformation zone (E_F) (friction zone)

$$E_F = 2\pi\,\sigma_0\,\mu\,t_0\,\Delta^2 \quad (14)$$

5- Total dissipated work (E_t)

$$E_t = 2\pi\sigma_o\, r_1{}^2 t_o\left(\frac{\Delta}{r_1} - \frac{2R_o - t}{2R_o - t_o}\sin\frac{\Delta}{r_1}\right) + 2\left(\frac{\pi\sigma_o\, r_1 t_o{}^2}{2}\sin\frac{\Delta}{r_1}\right) + 2\pi\sigma_o\,\mu\, t_o\Delta^2 \qquad (15)$$

Nosing load

$$P_n = 2\pi\sigma_o\, r_1 t_o\left[1 - \frac{2R_o - t}{2r_1}\cos\frac{\Delta}{r_1} - \frac{t_o}{2(R_o - t)}\tan^2\frac{\Delta}{r_1}\right] + \pi\sigma_o\, r_1\left[\frac{2tt_o}{R_o - t}\tan^2\frac{\Delta}{r_1} + \frac{t^2}{r_1}\cos\frac{\Delta}{r_1}\right] + 4\pi\sigma_o\,\mu\, t_o\Delta \qquad (16)$$

Where, r_1 is the initial mean radius, r_2 mean radius of the volume element, *t* is indicate wall thickness, R_o is outer radius of the tube, σ_o flow stress, Δ is axial displacement, E_t, E_c, E_B, E_u and E_F are the Dissipated work in hemispherical die.

FINITE ELEMENT (FE) SIMULATIONS

Finite Element Modeling

Plastic deformation of the tube nosing of an aluminum tube was adopted using an elasto-plastic FE simulation assuming anisotropic hardening and von-Mises yield criterion. The problem was accomplished using the ANSYS version 15 package. The FE tube mesh is an arrangement of 3125 (20-node) solid higher-order element (5 elements in the thickness direction, 25 elements in both axial and circumferential directions). Die/tube interface was modeled by 540 rigid surfaces and 625 flexible surfaces representing the tube outer surface, respectively 4290 elements and 15825 nodes were used.

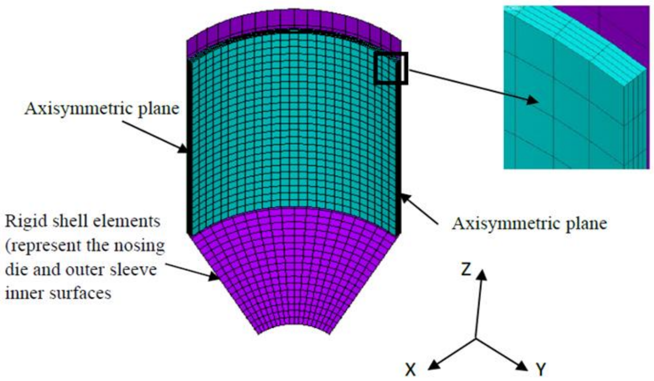

Fig. 3: FE model showing tube and conical die for tube nosing at semi-die angle 15 degree.

Considering the symmetric case in the nosing process, only a quarter of the tube and die were modeled. Perfectly rigid surfaces for both the punch and the die were assumed as an approximation. Figure 3 shows the 3-D tube mesh of an FE model for the tube nosing analysis. The friction law by Coulomb was used. The process was assumed to be carried out by moving the work-piece while the die is fixed. The nodes attaching tube end surface

were coupled to move in the nosing direction while the simulation was carried out applying the displacement to nodes along the Z-direction. Also, all the nodes on the side tube wall were considered fixed due to the presence of the symmetrical condition.

EXPERIMENTAL PROCEDURE

Commercial purity Aluminum was used as a work material. The original tube stock was received in the form of tubes 50 mm outer diameter and 5 mm thickness, cold-drawn supplied by the Egyptian Copper Factories Co. Alexandria, EGYPT. The tube specimens were machined on a center lathe with an outer diameter 48 mm. The specimens were finished with sandpaper. Table 1 shows the properties of the tubes and tube dimensions. Figure 4 schematic drawing of the tube nosing setup. A control sleeve was also utilized to constrain the tube. This modification is expected to eliminate bulging and avoid the occurrence of defects in the un-deformed part of the tube during the deformation process. Figure 5 shows the photo of the nosing setup on the test machine. Figure 6 gives the drawings of the used dies: conical dies with semi die angles of 15, 30, 45 and 60 degrees and the hemispherical die with 24.1 mm radius. Photos of manufactured nosing die, the newly designed punch and the control sleeve design are also shown in Figure 7. The nosing process was conducted using UNITED material testing system; (MTS), speed was 20 mm/min. Grease and PTFE were used as lubricants besides the dry condition. All experimental work was carried out at room temperature.

Table 1 Properties of the tubes and tube dimension.

Properties	Values
Outer tube diameter, D_o,mm	48
Initial tube length, L,mm	55
Wall thickness, t_o,mm	1, 1.5, 2, 2.5, 3, 3.5
Semi die angle,α,degree	15, 30, 45, 60
Coefficient of friction,μ	0.04, 0.05, 0.15
modulus of elasticity, E, GPa	70
Poisson ratio, ν	0.34
Strength coefficient, K, Mpa	135
Strain hardening exponent, n	0.24

RESULTS AND DISCUSSIONS

The theoretical analysis, finite element simulation and experimental work were conducted to study the effect of tube wall thickness, semi-die angle and coefficient of friction on load required to perform the tube nosing and the effect of die shape, nosing ratio, thickness and strain distributions on tube nosing process. This work based on assessment that compared the analytical prediction with numerical estimates obtained by finite element analysis and experimental work.

Effect of the coefficient of friction

Figure 8 presents the load/displacement curve in nosing of Al tubes in a conical die with semi die angle 15° and initial tube wall thickness 3 mm. From this curve, it can notice that load increase with increasing the coefficient of friction. There is good agreement between FE-prediction, theoretical and the experimental results.

Effect of the tube wall thickness

Figure 9(a, b, c) represent the load/displacement curves in nosing of Al tubes in a conical die with semi die angle 30° at different coefficient of friction. It can notice that load

increase with increasing the tube wall thickness. There is good agreement between FE-prediction, theoretical and the experimental results.

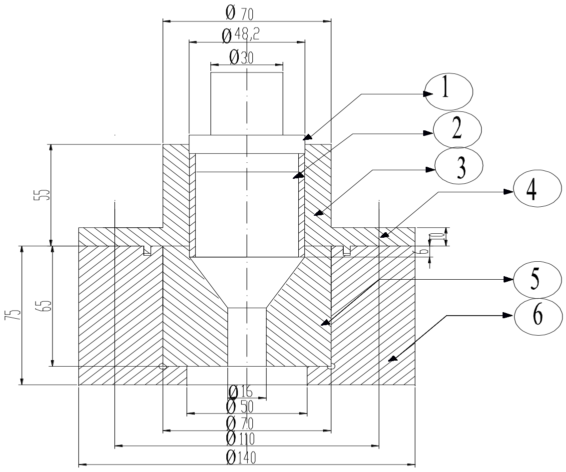

Fig.4: Nosing setup
1-Punch, 2- Specimen, 3- Control sleeve, 4- Bolt (4/90 °), 5- Nosing die, and 6- Die block.

Fig.5: Photo of the nosing setup on the MTS machine.

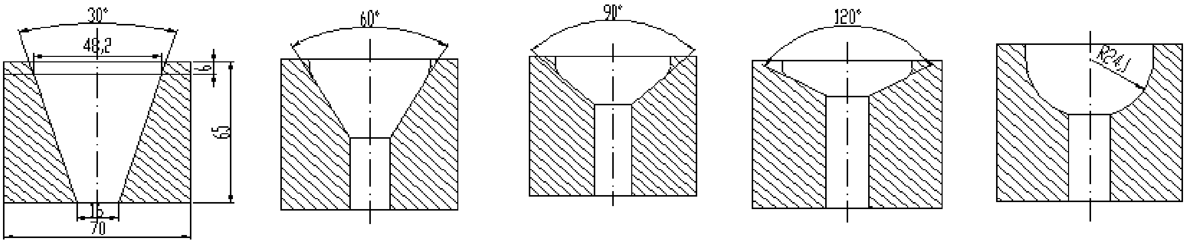

α= 15° α= 30° α= 45° α= 60° **Hemispherical die**

Fig.6: Schematic drawings of the tube nosing dies.

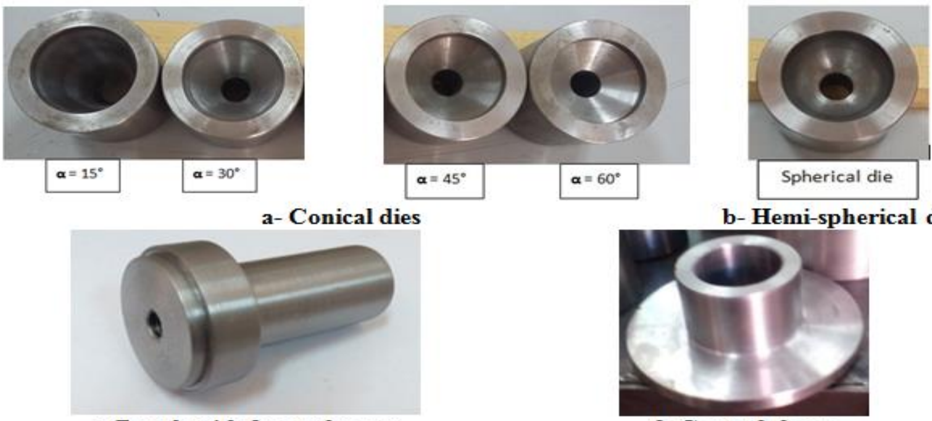

a- Conical dies **b- Hemi-spherical die**

c- Punch with front plunger **d- Control sleeve**

Fig. 7: Photos of manufactured dies, new designed plunger punch and control sleeve design.

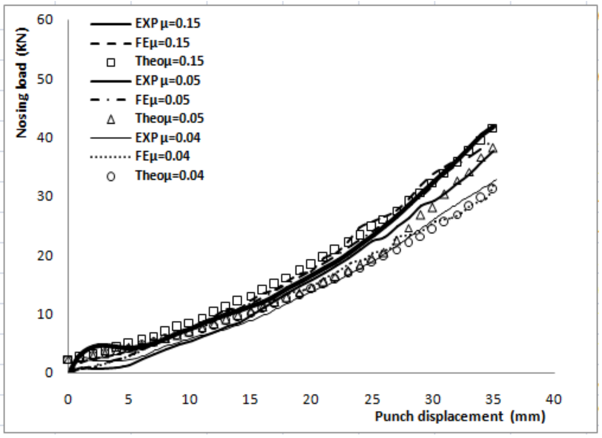

Fig.8: load/ displacement curve at different lubrication condition of the nosing tube.

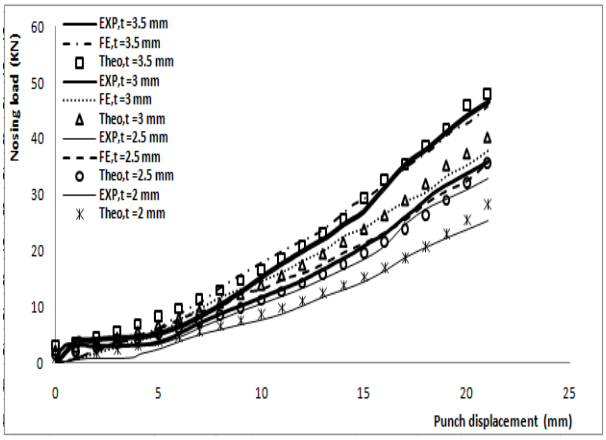

Fig.9a. load/ displacement curve at α=30°, and μ=0.15.

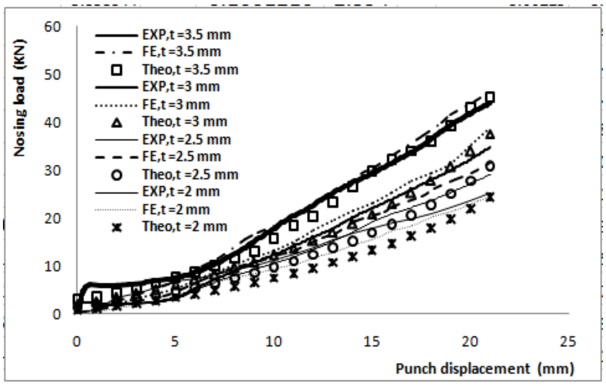

Fig.9b. load/ displacement curve at α=30°, and μ=0.05.

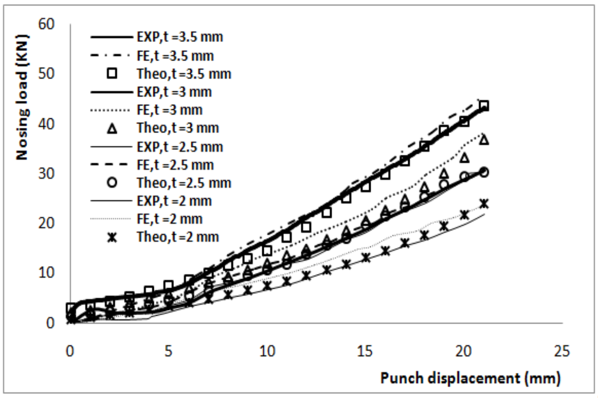

Fig.9c. load/ displacement curve at α=30°, and μ=0.04.

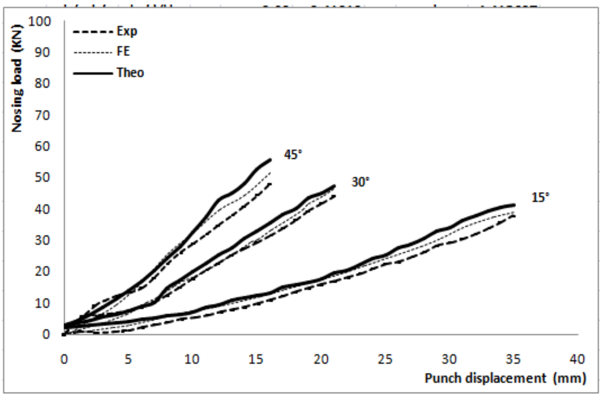

Fig.10 the influence of semi-die angles at lubricated condition (grease) of the nosing tube.

Die Shape

Effect of conical semi-die angle

Figure 10 shows the effect of different semi-die angles on load/displacement curve for thickness values of 3.5 mm and grease-lubricated specimens. The load required to finish the process is increased with increasing the semi-die angle at different displacement.

There is good agreement between theoretical results, FE-prediction and experimental results. Figure 11 shows specimens result after nosing process. At semi die angles 60°, it can be observed that the nosing process could not be completed because of folds occurred at leading edge.

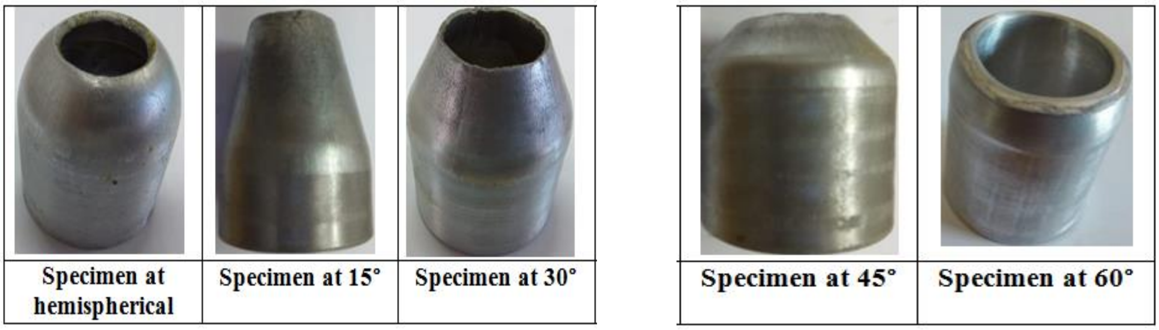

Fig.11 the deformed tubes after nosing process.

Effect of hemispherical die

Figure 12 and Figure 13 present comparison between FEM, theoretical analysis and the experimental work by using hemispherical die at coefficient of friction 0.05, and 0.04 respectively. The load increases with increasing the tube wall thickness. There were agreement between the FEM, theoretical and the experimental results.

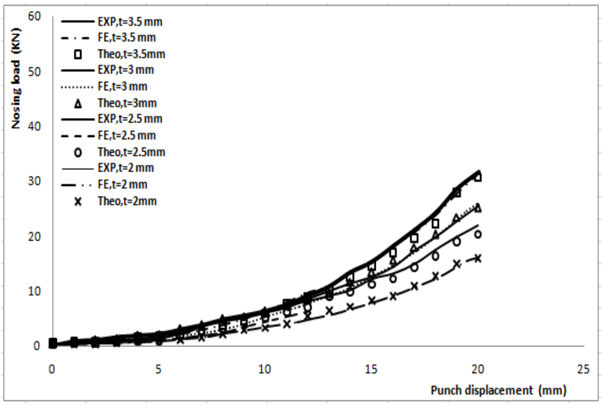

Fig.12 load/ displacement curve in hemispherical die at μ=0.05.

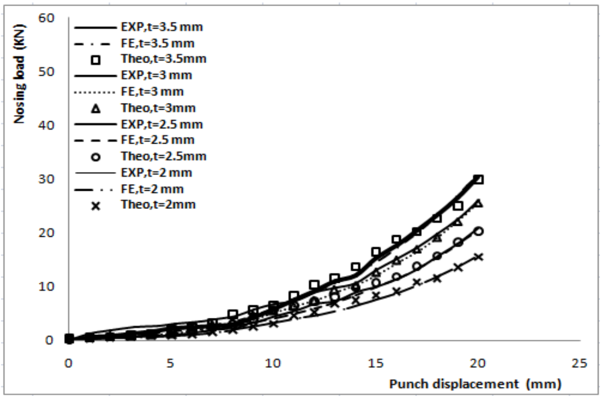

Fig.13 load/ displacement curve in hemispherical die at μ=0.04.

Effect of Nosing Ratio

Limiting nosing ratio (LNR): The deformation of a tube in nosing process can be evaluated by the nosing ratio (*NR*), which is defined as:

$$\eta = \frac{r_o - r_t}{r_o} \quad (17)$$

Where; η is the nosing ratio, r_t is the radius at the leading edge of the formed tube. There is a limiting nosing ratio (*LNR*), representing the largest reduction of tube throat that can be obtained without failure. The nosing ability of a metal tube depends on two factors:

1. The ability of the tube material to flow easily in the die cavity.

2. The ability of tube wall material to resist buckling.

Figure 14 shows the effect of tube wall thickness on nosing ratio at coefficient of friction is 0.05 in conical die with semi die angle 15°.The nosing ratio increases as wall thickness increases. Small wall thickness results in lower rigidity, which leads to the tube failure.

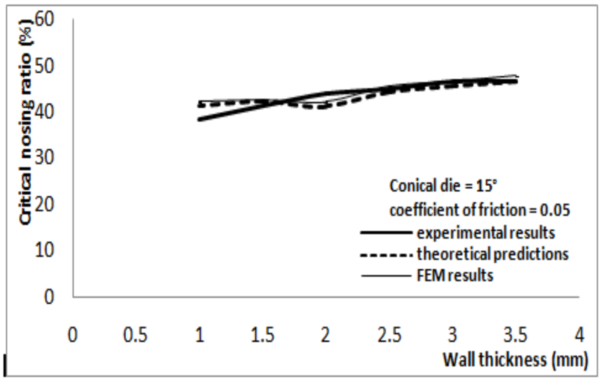

Fig. 14: Relationship between wall thickness and critical nosing ratio.

Effect of Die Penetration

Figure 15 shows the relationship between nosing ratio (r_t/r_o) and penetration ratio (h/ r_o). the theoretical calculation at different semi die angle (15°, 30°, 45°,60°) at coefficient of friction is 0.04 and wall thickness 2 mm. it can noticed that at low semi die angle the nosing ratio increase when the penetration ratio increase. Figure 16 presents the deformation state in FE simulation at punch strokes 35mm with semi-die angle 15°. From the deformation state, it shows the tube is smoothly nosed into the die.

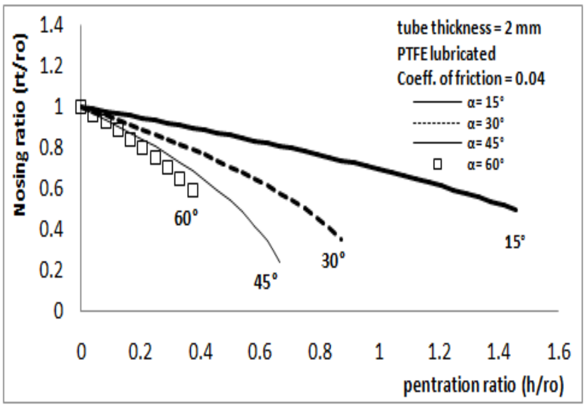

Fig. 15 the relation between nosing ratio (rt / ro) and penetration ratio (h / ro).

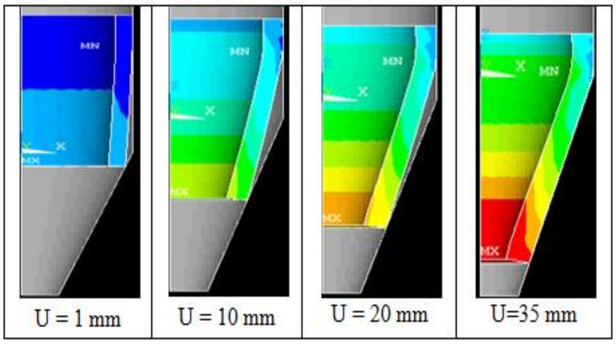

Fig. 16 deformation shape at different penetration at 15°.

Effect of strain distribution

The strain in tube end is considered had a great influence in success the nosing process. Figure 17 shows the strain distribution for the 55 mm aluminum tube under frictional conditions μ= 0.15 and μ= 0.04 at semi die angle 30° the distributions of axial strain ε_x, circumferential strain ε_θ and thickness strain ε_z are plotted. The sum of ε_x, ε_θ and ε_z were remaining zero for any distance from the base of the tube. It can observe that axial strain

ε_x gives negative value near the throat. This means that the deformed tube is shortened in this part. Figure 18 shows the effect of thickness distribution ε_z and ε_θ circumferential strain at tube wall thickness 3.5 mm at various semi die angle with different penetration for lubricated condition (μ = 0.05).it can observed that strain increase when the semi-die angle increases.

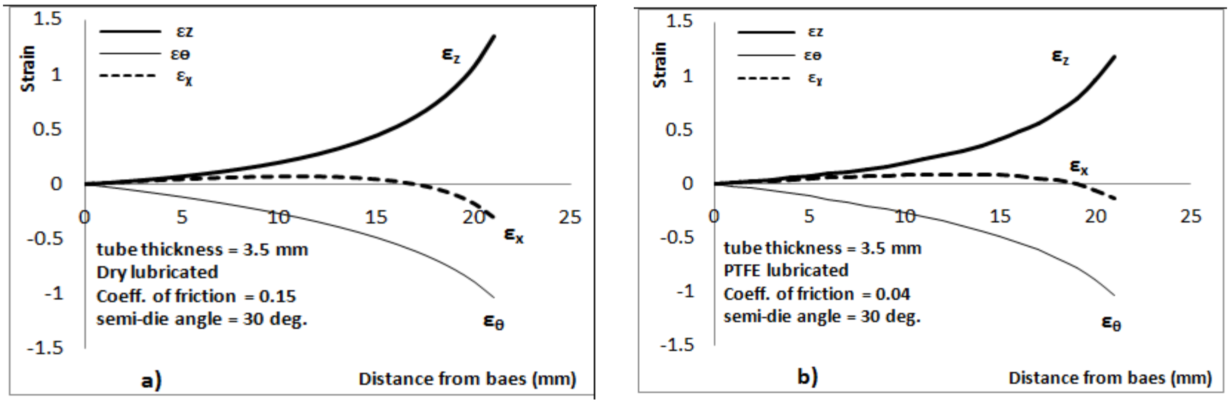

Fig.17. Strain distribution of nosed tube: a) μ = 0.15, b) μ = 0.04.

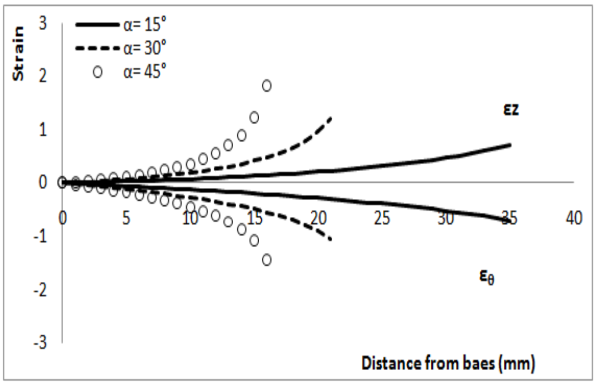

Fig. 18. shows the effect of thickness strain distribution at different semi die angle.

Effect of thickness distribution

Figure19 a, b shows the positions of thickness measurements on the nosed part and photo of the polished sliced part. Figure 20 shows the correlation between the FE-predicted and the experiment thickness of nosed part obtained for the values of tube wall thickness is 3.5 mm, semi-die angle of 15° and grease-lubricated condition. As shown from results, there is good agreement between FE, theoretical and experimental results.

Mode of failure in the nosed parts

FE- predicted folds and experimental ones appear in Figs. 21. It is clear that the agreement is excellent. From FE simulation and the experimental work, There is difficulty in conducting process the nosing the tube at semi-die angle 60° at different tube wall thickness.

For small thickness, wrinkling occurs in the nosed part in semi-die angle of 45°. This mode of failure occurs due to effect a combination of the increase compressive hoop stress Kuboki et al [19], and material anisotropy Tajally et al [16]. When the compressive stress at the smallest diameter of the nosed part reaches the critical value of the material, the wrinkle defect will appear, depending on the tube geometry, the die tube interface friction

condition and the semi die angle. FE- predicted wrinkles and experimental ones are appearing in Figure 22. It is clear that the agreement is very good.

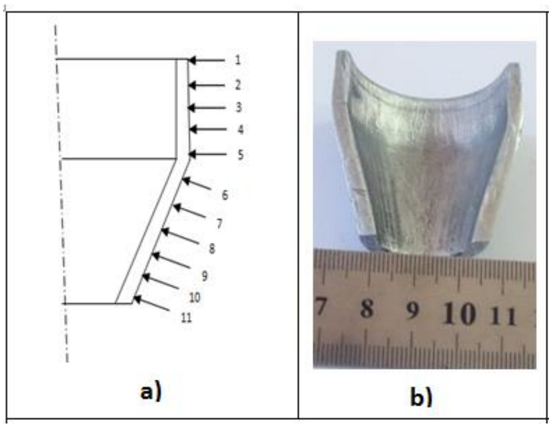

Fig. 19: a) shows the positions of thickness measurements on the nosed part b) photo of the polished sliced part at tube thickness 3.5 mm, semi-die angle 15°, and grease lubricated.

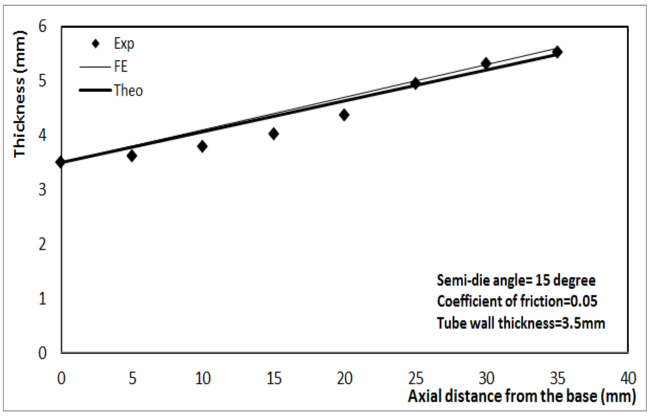

Fig. 20: Correlation between the FE-predicted and the experimentally values of thickness distribution, the values tube thickness 3.5 mm, semi-die angle15°, and grease lubricated.

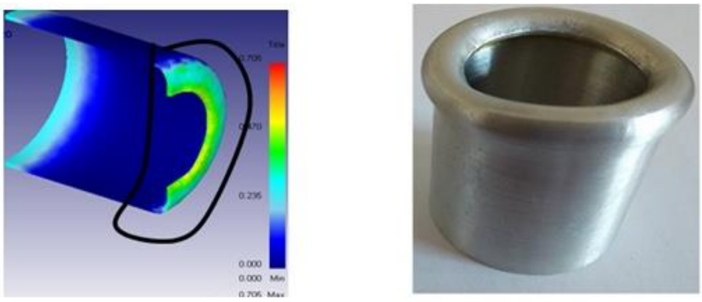

(a) (b)

Fig. 21: Folds occurred at conical die with semi-die angle 60° and wall thickness 1.5 mm. a) FE results, b) Experimental.

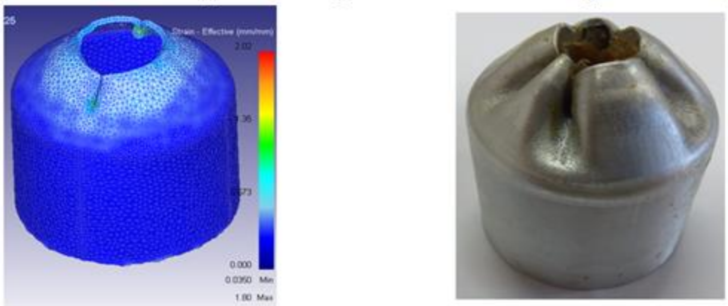

(a) (b)

Fig. 22: Wrinkling at conical semi-die angle 45°, wall thickness 1mm and grease-lubricated.
a) FE results, and b) Experimental

Earing occurs at the tip of the nosed portion of the tube at semi-die angle 15°, tube thickness 1 mm and grease-lubricated. This leads to form peaks and valleys at the tip of nosed part (ears) edges of the nosed part. Such ears decrease the yield of the tube. This depends upon the material anisotropy of nosed tube such as in deep drawing and ironing operations Tajally et al [16], Figure 23 a, b shows the FE-predicted and experimental ears developed when nosing in a conical die, semi-die angle 15°, wall thickness 1mm and grease-lubricated respectively. The similarity between the two results is clear, indicating a good agreement.

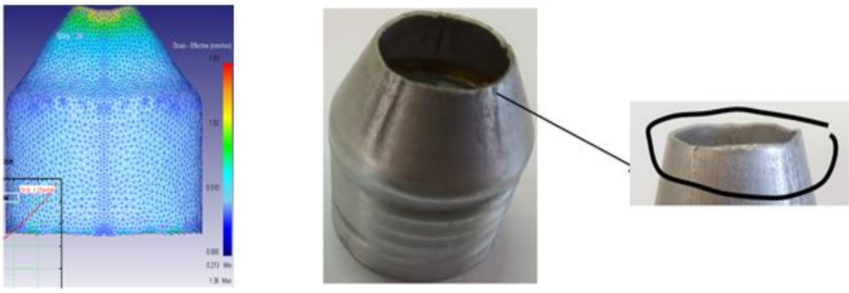

(a) (b)

Fig. 23: Earing at conical semi-die angle 15°, wall thickness 1mm and grease-lubricated. a) FE results and b) Experimental.

CONCLUSIONS

From the theoretical analysis, FE simulation predictions and the experimental results of commercial purity aluminum tube nosing process into both conical and hemispherical dies using an advanced design, the following conclusions may be found from this study:

1- **Theoretical analysis provides a simple way to predict the nosing load, thickness and strain distributions.**
2- **Results from theoretical and FE data on load /displacement curves are in agreement with the experimental results in both conical and hemispherical dies.**
3- **The nosing load in dry condition gives high values than in grease lubricated and PTFE lubricant.**
4- **For conical dies, results showed that forming loads increased by increasing the tube wall thickness and semi-die angle. For hemispherical die, results showed that forming loads increased by increasing the tube wall thickness and coefficient of friction. Experimental nosing ratio proved to increase by increasing the tube thickness.**
5- **Wrinkling, folds and ears formation defects were successfully modeled by the FE simulation and verified by the experimental results. Wrinkling occurs at thin thickness, folds occurs at large semi-die angle, and ears occurred at thin thickness.**
6- **Bulging defect could be eliminated with the use of the modified punch and constrained sleeve design.**

ACKMOWLEDGEMENTS

The authors declare that they have no conflict of interest. No fund from any organization was relieved in any form. The experimental work described in this paper was performed at the Material Forming Lab, Faculty of Engineering, Minia University, Minia EGYPT. Thanks are due to Nour-Elhoda Hussein, the Lab engineer for her help in conducting the experiments.

REFERENCES

1. Zhu J. A., "New approach to perform design in shell nosing", J Mater Processing Technol 63: pp. 640 - 644, (1997).

2. Kobayashi S., "Approximate solutions for perform design in shell nosing", Int J Mach Tool Des Res 23 (2/3): pp. 111–122, (1983).

3. Tang M. C., Hus M., Kobayashi S., "Analysis of shell nosing process mechanics and perform design.", Int J Mach Tool Des Res 22 (4): pp. 293–307, (1982).

4. Alves L. M., Pardal T. C. D., Martins P. A. F., "Nosing thin-walled tubes into axisymmetric seamless reservoirs using recyclable mandrels", J Cleaner Prod 18: pp. 1740–1749, (2010).

5. Alves L. M, Pardal T. C. D., Martins P. A. F., "Forming of thin-walled hollow spheres using sacrificial polymer mandrels", Int J Mach Tools Manuf 49: pp. 521–529, (2009).

6. Kwan C. T., Fang C. H., Chiu C. J., Chen S. W., Wen H. W., "An analysis of the eccentric nosing process of metal tubes. Int J Adv Manuf Technol 23: pp. 190−196, (2003).

7. Lu Y. H., "Study of preform and loading rate in the tube nosing process by spherical die", Comput Methods Appl Mech Engrg 194(25-26): pp. 2839–2858, (2005).

8. Huang Y. M., "Flaring and nosing process for composite annoy tube in circular cone tool application", Int J Adv Manuf Technol 43(11-12): pp. 1167–1176, (2009).

9. Gouveia B. P. P., Alves L. M., Rosa P. A. R., Martins P. A. F., "Compression beading and nosing of thin- walled tubes using a die: experimental and theoretical investigation", Int j mech Mater Des 3(1): pp. 7–16, (2006).

10. Kuboki, T., Kimura, Y., Murata, M., Shimoda T., "Tool design for suppressing fracture at the tip of tube after nosing with die", International Conference on Computational Plasticity, pp. 1-4, (2005).

11. Huang, Y. M., Yuung, H. L., Chen, M. C., "Analyzing the cold-nosing process using elasto–plastic and rigid–plastic methods", Journal of Materials Processing Technology, 30, pp. 351–380, (1992).

12. Rosa, P. A. R., Rodrigues, J. M. C., Martins, P. A. F., "External inversion of thin-walled tubes using a die: experimental and theoretical investigation", International Journal of Machine Tools & Manufacture, 43, pp. 787–796, (2003).

13. Rotter, J. M., Sadowski, J. A., Chen, L., "Nonlinear stability of thin elastic cylinders of different length under global bending", International Journal of Solids and Structures, 51, pp. 2826–2839, (2014).

14. Salih D. S. M, Ismail A. R., "Investigation die profile effect on nosing process using finite element method", Modern Appl Sci 5 (2), pp. 212–222, (2011).

15. Manabe K. I., Nishimura H., "Improvement of forming limit in conical nosing of thin walled tubes", Bulletin of JSME, 28 (245-32): pp. 2730–2736, (1985).

16. Tajally M., Emaddodin E., Qods F., "An experimental study on earing and planar anisotropy of low carbon steel sheets", World Appl Sci J 15(1): pp. 1-4, (2011).

17. Mohammed M. A. Y., "Theoretical and experimental study on nose forming of metallic tubes", M. Sc. Thesis, Assiut University, Assiut, pp. 35–47, (2003).

18. Amirhosseini S. G., Niknejad A., Setoudeh N., "Nosing process of empty and foam-filled circular metal tubes on semispherical die by theoretical and experimental investigations", Trans Nonferrous Met Soc China 27: pp. 1976−1988, (2017).

19. Kuboki T., Abe M., Yamada Y., Murata M., "Flexible rotary reduction of tube tips by dies with relief surfaces for attaining high forming limit and productivity.", CIRP Ann—Manuf Technol 64: pp. 269–272, (2015).